

## Spiral wave drift induced by stimulating wave trains

Georg Gottwald, Alain Pumir, and Valentin Krinsky  
 INLN, 1361, Route des Lucioles, F-06560, Valbonne, France

(Received 25 January 2001; accepted 25 June 2001; published 22 August 2001)

We investigate the drift of a spiral wave core in a homogeneous excitable medium under the influence of a periodic stimulation by wave trains close to the core. Two important results were found. First, as opposed to existing theories of spiral wave drift, we observe drift induced by wave trains with periods larger than the period of the freely rotating spiral wave. Second, when investigating the drift of meandering spirals we found that the property of meandering of spirals is not robust against periodic stimulations. Simple phenomenological arguments are provided to explain these observations. © 2001 American Institute of Physics. [DOI: 10.1063/1.1395624]

**Rotating vortices in cardiac muscle induce numerous cardiac disturbances. The most severe, fibrillation, results in chaotic contractions [see the Focus Issue “Fibrillation in Normal Ventricular Myocardium” in *Chaos* (1998)]. Ventricular fibrillation induces clinical death in ~1 min. Fibrillation can be arrested by a strong electric discharge called defibrillation, which kills all propagating waves in myocardium, albeit with undesirable side effects. An alternative approach consists in forcing rotating vortices to drift and to annihilate at the boundaries of the excitable tissue. This can be done clinically with trains of electric pulses. In this work, we investigate this process with the help of a simplified mathematical model. Previous works had found that the rotating wave cannot drift, unless some restricting conditions are imposed on (i) the frequency of the stimulating fronts and on (ii) the excitability of the medium, imposing important clinical limitations. We show here that these two conditions can be (partially) relaxed. We give numerical evidence, and develop a phenomenological model to support our conclusions.**

### I. INTRODUCTION

Many chemical and biological systems exhibit excitability. In two-dimensional systems excitable media typically give rise to spiral waves.<sup>1-3</sup> The study of spiral waves is particularly important from a medical point of view as they are believed to be responsible for pathological arrhythmias of the heart. A dangerous class of arrhythmias are the reentrant arrhythmias, in which the same wave of excitation repeatedly reinvades the same piece of tissue; these reentrant arrhythmias are high frequency, as the period of the reentrant wave is less than the normal period of the heartbeat, and underly atrial flutter and monomorphic ventricular tachycardia. If reentrant waves break down, due to their intrinsic instability, or the effects of anisotropy and the geometry of the heart, spatio-temporal irregularity in the pattern of activation produces a dangerous stimulation, in which different parts of the same chamber of the heart are activated at different times. Global coordination of the contraction of the heart is lost, and, instead of pumping rhythmically and

firmly, the heart writhes and quivers. The circulation is no longer maintained and death can result if the heart is not defibrillated. Immense research goes into studying defibrillation, which is the medical treatment to stop lethal fibrillations of the heart. The most widely used method is to apply a high-voltage transthoracic electric shock (usually about 5 kV, 20 A for a duration of 2–5 ms) to force the heart back to its resting state so that the pacemaker, the sinoatrial node, may start again in a controlled fashion. Although successful, this method is very damaging to the heart tissue, so there is a need to look for different, less harmful methods. One promising approach is an implantable device of a new type which detects arrhythmias similarly to a standard implantable defibrillator, but instead of sending a strong electric shock, it shoots fronts towards a spiral wave to move its center of rotation. The wave train may successively annihilate the spiral wave arms, and penetrate to the core where the pulses can now directly interact with the spiral wave tip.

Spiral wave drift, induced by periodic wave trains, has been observed in excitable media<sup>4</sup> and has been theoretically described.<sup>4-6</sup> The two existing theories for spiral wave drift induced by periodic wave trains focus on two extreme areas in the parameter space in terms of the density of the spiral. The density  $\delta$  of a spiral can be defined as the ratio of the width of the spiral wave arm and the wavelength of the spiral wave. In other words, the density is a measure of the ratio of the space already occupied by the spiral to the space that would still be available for excitations. No theoretical analysis has been done for the intermediate range.

We briefly recall here the essential ideas put forward in these papers.

In the extremely sparse case it is assumed that after every collision of a stimulating pulse with the spiral wave tip, the hereby created broken end will immediately start curling and the tip will move on a circle whose radius is the one of a freely rotating spiral wave. The resulting drift will be a cycloid consisting of the originally freely rotating spiral. The explicit formulas for the drift velocities in the  $x$ - and  $y$ -components ( $c_{d_x}$  and  $c_{d_y}$ ) of the total drift velocity ( $c_d$ ) read

$$c_{d_x} = \frac{R(\cos(\omega T_c) - 1)}{T_c}, \quad c_{d_y} = \frac{R \sin(\omega T_c)}{T_c}, \quad (1)$$

where  $\omega$  is the frequency of the spiral wave and the collision time  $T_c$  is implicitly given by

$$c_f(T_c - T_f) = R \sin(\omega T_c), \quad (2)$$

where  $T_s$  is the rotation period of a freely rotating spiral wave and  $T_f$  is the stimulation period by which wave trains traveling with velocity  $c_f$  are emitted towards the spiral. Note that a spiral may actually drift towards the periodic wave train, as can be seen from Eq. (1).

In the extremely dense case it is assumed that the excitability is so large that one may neglect curvature effects. Here one has to take into account recovery periods due to the inhibitor during which the broken end moves upwards with the front velocity  $c_f$  before it can curl again to meet the next planar pulse. This leads to

$$c = c_f \left( 1 - \frac{T_f}{T_s} \right). \quad (3)$$

Note that, contrary to Eq. (3) for dense spirals, which depends only on  $T_s$ , Eq. (1) requires the knowledge of one more parameter, i.e., the radius of the core  $R$  (the velocity of the spiral wave tip  $c_s$  is given then as  $2\pi R/T_s$ ).

Both theories state that drift is not possible for wave trains with a stimulation period  $T_f$  larger than the period of the spiral wave  $T_s$ .

This result is based on the following general collision argument. Contrary to many other waves, waves in an excitable medium annihilate each other when colliding. If the period  $T_s$  of a spiral is smaller than the period of the wave train  $T_f$ , the core will never be influenced by the stimulation when the location of the stimulation is far from the core. The spiral wave arms shield the core. For periods smaller than  $T_s$  the spiral wave arms and the wave train will annihilate each other until the wave train will have penetrated to the core where it will induce drift.

The maximal stimulation period  $T_s$  was considered to be a universal law and, from a clinical point of view, imposes limitations of this approach for an implantable device, since it requires damaging high frequencies.

In this work we demonstrate that, contrary to classical belief, smaller stimulation frequencies may be used to induce drift in an excitable medium. The reason for the differing observation between the classical result and our result appears to be twofold. First, we leave the extreme regions in the density parameter range and instead investigate moderately sparse spirals. Second, we look at stimulations close to the core whereas, in previous theories, the stimulation source is assumed to be located far from the core. For stimulation close to the core it was well known that a single stimulating pulse may displace the spiral wave core. But constant nonzero drift velocities for  $T_f/T_s > 1$  have never been investigated and observed before. The apparent contradiction with the collision argument can be explained by the fact that the spiral *increases* its effective period by interacting with the wave train, so the new period  $T_s^*$  satisfies  $T_f/T_s^* < 1$ .

Interestingly, we also find that meandering of spirals is not robust against periodic stimulations and that meandering spirals exhibit drift in the same way as nonmeandering spirals.

Drift along a straight line was previously observed and studied in an inhomogeneous medium,<sup>7,8</sup> or under a periodic modulation of the properties of the medium (see for example Refs. 9–11). In many cases drift along a straight line is not generic, but instead only occurs for one value of a control parameter which leads to a resonance of the forcing frequency and the spiral wave period  $T_s$ . This is very different for stimulation with wave trains which we will discuss here where the drift along a straight line is the generic case.

In Sec. II we introduce the model under investigation and the numerical methods used. In Sec. III we present our result that nonzero drift velocities can actually be obtained for larger stimulation periods. In Sec. IV we provide a new general approach to combine the two classical theories. In Sec. V we investigate the seemingly paradoxical result of nonzero drift velocities, and a phenomenological formula describing drift will be given. In Sec. VI we will study the drift of meandering spirals under the influence of a stimulation close to the core. The results and their clinical implications are discussed in Sec. VII.

## II. MODEL AND NUMERICAL METHODS

We briefly present here the model studied, and the numerical methods used in this work.

### A. Theoretical model

We investigate a two-component two-dimensional excitable medium with an activator  $u$  and a nondiffusive inhibitor  $v$  of the following form:

$$\begin{aligned} u_t &= \Delta u + u(1-u)(u-(v-b)/a), \\ v_t &= \epsilon(u-v), \end{aligned} \quad (4)$$

introduced by Barkley.<sup>12</sup> Here  $\Delta$  represents the two-dimensional Laplacian, and  $a$  and  $b$  and  $\epsilon$  measure the excitability and refractoriness. As a general rule, increasing of  $a$  and/or decreasing of  $\epsilon$  will move the parameter range towards denser spirals. We analyze a homogeneous medium without defects to which a drifting spiral may pin<sup>13–15</sup> and unpin.<sup>16,17</sup>

We study the emission of planar wave trains onto a spiral wave as depicted in Fig. 1. Here we look at stimulations close to the core and measure the drift velocity as a function of the stimulation period  $T_f$ .

### B. Numerical method

For the integration scheme we used the method described by Barkley.<sup>12</sup> Most of the numerical simulations were performed in a box of length  $L=30$ , grid-size  $dx=0.2$ , and time stepping  $dt=0.1$ .

The initial condition was constructed by combining a stationary traveling front, and a steadily rotating spiral wave, as seen in Fig. 1. One difficulty in preparing the initial condition is to avoid multiple broken ends, caused by the interaction of the wave trains with the inhibitor field,  $v$ . This leads to very long transients and to a waste of computer resources. This problem is very severe when the spiral is dense; for this reason, we restricted ourselves to moderately sparse spirals. Also, we artificially set initially the inhibitor

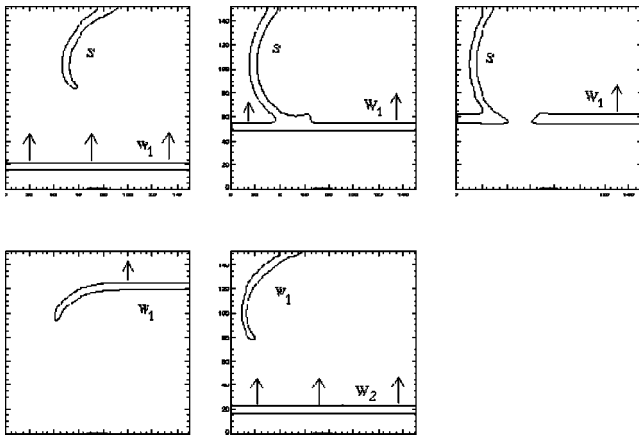


FIG. 1. Dynamics of a spiral wave  $S$  induced by a wave train  $W_{1,2}$ . The activator  $u$  is shown. The time increases from left to right. (a) A planar front  $W_1$  is sent towards a spiral wave arm  $S$ . (b) Shortly after the collision. (c) Broken front  $W_1$  is created. (d) Broken end  $W_1$  evolves into a new spiral wave arm. (e) The next pulse  $W_2$  of the stimulating wave train is launched. The wave pattern is similar to (a), but the spiral wave appears shifted.

field of the spiral wave to zero where the stimulating front is about to run into the rotating wave. We have checked that this somewhat *ad hoc* way of preparing the solution does not affect the value of the drift velocity, by comparing the results obtained for different preparations of the initial conditions. In the absence of external stimulation, the artificially truncated initial condition evolves into a freely rotating spiral with the same spiral wave core.

Due to the limited size of the computational domain, the core of the spiral wave is very quickly pushed away from the numerical box, before a steady regime can be observed. This difficulty can be avoided by adding a drift term:  $-c_{dx}u_x - c_{dy}u_y, -c_{dx}v_x - c_{dy}v_y$  to the left-hand sides of Eqs. (4). This enables us to investigate the long-time behavior of the spiral wave drift. The drift velocities  $c_{d,x,y}$  were determined during the numerical integration, by taking the ratio between the observed displacement and the time it takes between two consecutive minima of the  $x$ -coordinate of the trajectory of the tip.

In the problem we are considering, the frequency of the stimulation must be fixed in the laboratory frame. Because a moving frame is used for numerical purposes, one has to properly take the Doppler shift into account. This is done in practice by adjusting the stimulation period in the moving reference frame,  $T_{f,num}$ , so as to maintain the wavelength of the stimulating pulse constant. Note that the stimulation wave comes from the lower side of the numerical box (see Fig. 1).

We checked that the result was very robust with respect to the precise choice of the parameters.

We used Neumann no flux boundary conditions. It is well known that in this case the wave may exhibit drift due to its interaction with its mirror image (see, for example, Ref. 18 for resonant drift). It has been checked by comparing the numerical results for different initial positions of the spiral core that the drift is not due to this boundary effect.

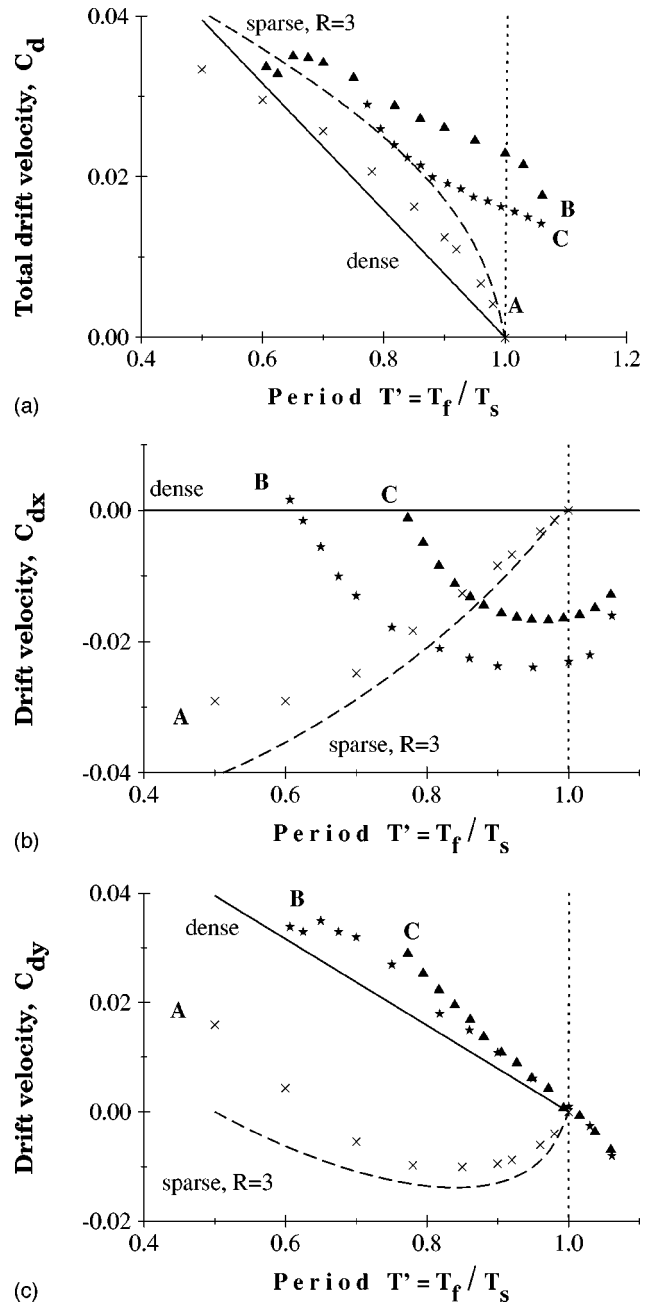


FIG. 2. Drift velocities. (a) total drift velocity  $c_d$ , (b)  $x$ -component  $c_{dx}$ , (c)  $y$ -component  $c_{dy}$  versus  $T' = T_f/T_s$ . The two continuous lines show the theoretical limits for sparse spirals, Eq. (1) (here arbitrarily chosen  $R = 3$ ), and dense spirals, Eq. (3). The crosses, stars, and triangles are numerical simulations A, B, and C. The density of the spiral increases from A to C. To the right of the vertical line at  $T' = 1$  both theoretical limits predict that there is no drift at all. Our numerical results show a nonzero drift in this region. Parameters are  $b = 0.005, D = 0.02, \epsilon = 0.02, L = 30$ , and  $a = 0.29$  for case A,  $a = 0.32$  for case B, and  $a = 0.4$  for case C. Case A is almost a sparse spiral behaving according to (1), case B is a moderately sparse spiral, and the parameters of case C support a meandering spiral. The coincidence of the  $y$ -components of the drift velocity in (c) for cases B and C is accidental.

### III. RESULTS

Figures 2(a)–2(c) shows the dependence of the drift velocity on the nondimensionalized stimulation period  $T' = T_f/T_s$ . It is clearly seen that nonzero drift velocities exist for  $T' \geq 1$ , contrary to the existing theories. We give ex-

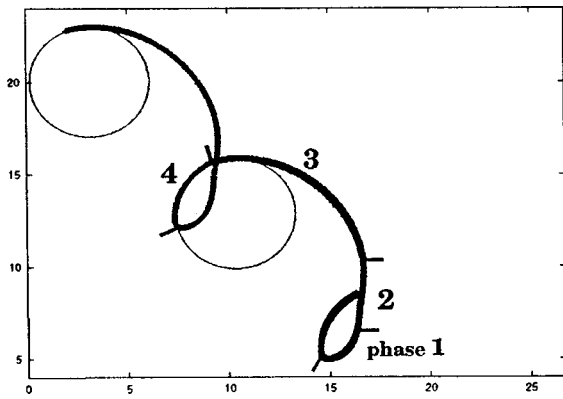


FIG. 3. Spiral wave tip movement during stationary drift (thick line). Superimposed is the core of a freely rotating spiral (thin line). Parameters are the same as in case B in Fig. 2.

amplitudes for sparse nonmeandering spirals (case A), moderately sparse nonmeandering spirals (case B), and moderately sparse meandering spirals (case C).

Our numerical results face us with a paradox: on the one hand, general collision arguments tell us that nonzero drift velocities cannot be observed for  $T_f/T_s \geq 1$ ; on the other hand, we clearly observe nonzero drift velocities for  $T_f/T_s \geq 1$ . The core of our argument to resolve the paradox is that the trajectory of the spiral wave tip after the collision results in an effectively larger spiral wave period  $T_s^*$ . To understand this we will look in the following paragraph into the actual dynamics of the spiral wave trajectory after the collision.

As Fig. 3 shows, there are mainly four phases for moderately sparse spirals, an initial collision phase (phase 1 in Fig. 3), a noncurling phase due to a strong “dense” interaction of the broken front with the refractory tail of the spiral (phase 2 in Fig. 3), then a transitory curling phase (phase 3 in Fig. 3) and a fourth phase where the spiral wave tip eventually has relaxed onto the core of a freely rotating spiral (phase 4 in Fig. 3).

During the noncurling phase 2 the newly created broken end and the next wave train are almost moving without changing their distance due to the refractoriness and, hence, the tip velocity is  $c_f$ .

Despite the transitory nature of phase 3 where the spiral has not yet relaxed on the stationary core, the numerics show that its velocity has already reached the stationary velocity  $c_s$ . This is the two-dimensional analog of the observation in one dimension that arbitrary initial conditions very quickly assume the stationary velocity although their shape has not taken the stationary shape. This is due to the fact that the velocity is determined by diffusion and hence only the foremost part of the front does matter. It is this transitory phase 3 which has been neglected so far and which allows for nonzero drift velocities for  $T' > 1$  (in Ref. 5 only phase 4 has been considered, and in Ref. 4 only the noncurling phase 2 has been considered under the assumption of equal growing and front velocities). During phase 3 the tip moves on a quasi-circle with a radius larger than the radius of the freely rotating spiral, as can be seen in Fig. 3. This effectively introduces a larger spiral wave period  $T_s^* > T_s$  to keep the velocity  $c_s$  constant. This explains the seemingly paradoxical

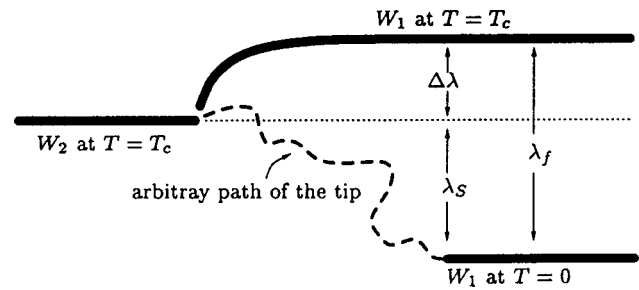


FIG. 4. Sketch of a broken front  $W_1$  at  $T=0$ . It evolves into a spiral  $W_1$  at  $T=T_c$ .  $W_2$  is the next wave train which collides with the spiral at  $T=T_c$ .

nonzero drift velocities for  $T' = T_f/T_s \geq 1$  since the results in Fig. 2 are depicted versus the spiral wave period of the freely rotating spiral  $T_s$ .

Studying the dependence of the drift velocity on the initial conditions in terms of position of the spiral wave tip on the core of the freely rotating spiral, we found the plausible result that the actual values of the drift velocities do not depend on the initial conditions, but that the maximal  $T' \geq 1$  exhibiting nonzero drift velocities does depend on the initial conditions. This is not surprising because the initial position of the spiral wave tip relative to the position of the wave train determines how well the spiral wave is shielded. The longer it takes for the first collision the more  $T'$  tends to the classical result  $T'=1$  with the important difference, though, that the drift velocity is nonzero.

We note that the numerical results for small  $T_f/T_s$  become unreliable since the period of the wave train  $T_f$  is not big compared to the minimal period for the existence of wave trains  $T^*$  and the excitability is not homogeneous along the front, but instead the fronts will be wiggly after the interaction.

In Sec. V we will employ a more quantitative understanding of the drift velocities, but first we briefly review the classical theory.

#### IV. CLASSICAL THEORY REVISED

The idea that spiral waves may drift as a result of an interaction with a wave train has been first proposed in two seminal papers.<sup>4,5</sup> The two limiting cases of very dense spirals<sup>4</sup> and very sparse spirals<sup>5</sup> were studied in detail.

In the following we will present a simple but general view on the mechanism of drift which includes the extremely sparse case<sup>5</sup> as well as the extremely dense case.<sup>4</sup> Suppose a spiral and a planar front meet at  $T=0$  (see Fig. 4) to form a broken end  $W_1$  [as in Fig. 1(d)]. The wave train far from the tip will continue its movement with the velocity  $c_f$ , whereas the tip will have its own individual path with typically a velocity smaller than  $c_f$ . At a later point in time  $T_c$  the wave front  $W_1$  will have traveled  $\lambda_f = c_f T_c$  and the spiral wave tip will have traveled  $\lambda_s = \int_0^{T_c} v_y dt$ , where  $v_y$  is the y-component of the tip velocity during its drift. The two waves  $W_1$  and  $W_2$  have the constant distance  $\Delta\lambda = c_f T_f$ . If we take  $T_c$  as the time of collision after which the spiral tip of  $W_1$  and  $W_2$  meet to form another broken end, we obtain  $\Delta\lambda = \lambda_f - \lambda_s$  (see Fig. 4) and, therefore,

$$c_f T_f = c_f T_c - \int_0^{T_c} v_y dt, \tag{5}$$

and for the drift velocities

$$c_{d_x} = \frac{\int_0^{T_c} v_x dt}{T_c}, \quad c_{d_y} = \frac{\lambda_S}{T_c} = c_f \left( 1 - \frac{T_f}{T_c} \right). \tag{6}$$

Generally it is hard to determine  $v_{x,y}$  and to obtain analytical evaluations of these formulas. But for extremely sparse and extremely dense spirals one can make assumptions about the form of  $v_{x,y}$  and the collision time  $T_c$  and obtain the previous results (1), (2), or (3), respectively.

It is readily seen that Eqs. (5) and (6) imply the extremely sparse case (1) and (2) if one assumes that the path of the tip will be the one of a freely rotating spiral, i.e., assuming  $v_x = -c_f \sin(\omega T)$ ,  $v_y = c_f \cos(\omega T)$  and requiring for the velocity of the spiral wave  $c_s = c_f$ .

In the extremely sparse case the underlying assumptions are that the refractoriness of both spiral and wave train can be neglected. In particular, there is no interaction of the front and the spiral wave arm with the refractory tails of each other, implying that the period of the wave train  $T_f$  as well as the spiral wave period  $T_s$  are big compared to the minimal period of a wave train  $T_{min}$ . Also interaction of the pulse with the spiral wave core is neglected and, furthermore, the core radius  $R$  of the spiral wave is assumed to be sufficiently large so that curvature effects can be neglected, or, in other words, the velocity of the spiral at the core  $c_s = 2\pi R/T_s$  is equal to the velocity of a planar wave  $c_f$ .

The general approach (5) and (6) allows us as well to recover Eq. (3) for extremely dense spiral waves. For dense spirals we assume  $T_c = T_s$  and neglect the drift in the  $x$ -direction. This essentially means that the drift caused by the refractoriness of dense spirals is dominating over the curling and that the excitability is so high that the velocity of the spiral is  $c_f$ .

Equations (5) and (6) are general equations and imply the simple cases of extremely sparse and dense spirals. But as soon as the dynamics involves a more complicated structure, it is hard to find an analytical expression for  $v_x$  and  $v_y$ , based on some simple assumptions. Therefore, we employ a different phenomenological approach in the next section to explain the nonzero drift velocities we observe for moderately sparse spirals.

### V. PHENOMENOLOGICAL MODEL

We introduce here a phenomenological ansatz for the drift velocities for moderately sparse spirals. In Fig. 5(a) we sketch the basic idea. We replace the actual trajectory of the tip (continuous line) with an equivalent motion (dashed line) with the same initial and final coordinates A and C. The reduced motion consists of a linear movement AB and a motion on the circle BC. Here,  $\vartheta$  determines the initial position of the tip on the core and  $T_c^*$  the final position. The dimensional ‘‘angle’’  $\varphi$  determines the position of the spiral wave at the time of collision relative to the incident wave

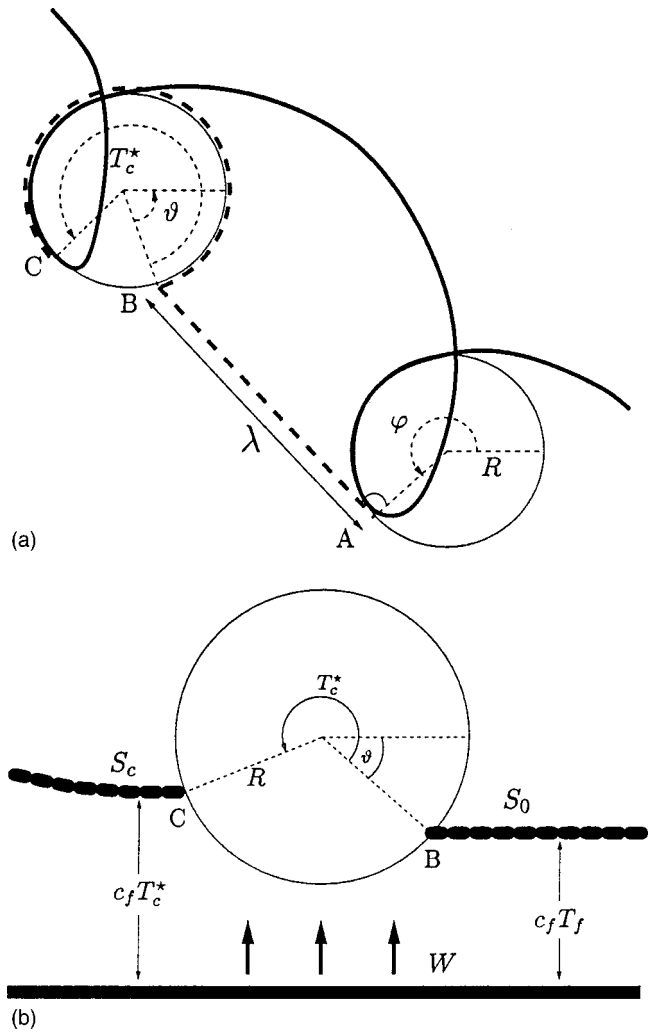


FIG. 5. (a) Illustration of the phenomenological model. (b) Close-up of the tip motion on the circle CB.  $S$  is a spiral wave arm moving along the core with radius  $R$ .  $W$  is a stimulating wave train.  $S_0$  is the spiral wave at the start of its travel time along the core.  $S_c$  is the same spiral wave arm at the time of collision.

train, i.e.,  $\varphi = T_c^* - \vartheta$ . The displacement of the circles is determined by  $\lambda$ . The total displacement during the time between two collisions is given by [Fig. 5(a)]

$$D_x = R(\cos(\omega \varphi) - \cos(\omega \vartheta)) + \lambda \sin(\omega \varphi), \tag{7}$$

$$D_y = R(\sin(\omega \varphi) - \sin(\omega \vartheta)) - \lambda \cos(\omega \varphi). \tag{8}$$

The time between two collisions  $T_c$  consists of the time of the movement along the circle BC and along the straight line AB. Since the tip displacement along AB is due to the stimulating front (phase 2) which propagate in the  $y$ -direction we may write for the total collision time

$$T_c = T_c^* - \frac{\lambda}{c_f} \cos(\omega \varphi). \tag{9}$$

Therefore, the drift velocities are given by  $c_{d_x} = D_x/T_c$  and  $c_{d_y} = D_y/T_c$ , which reads as

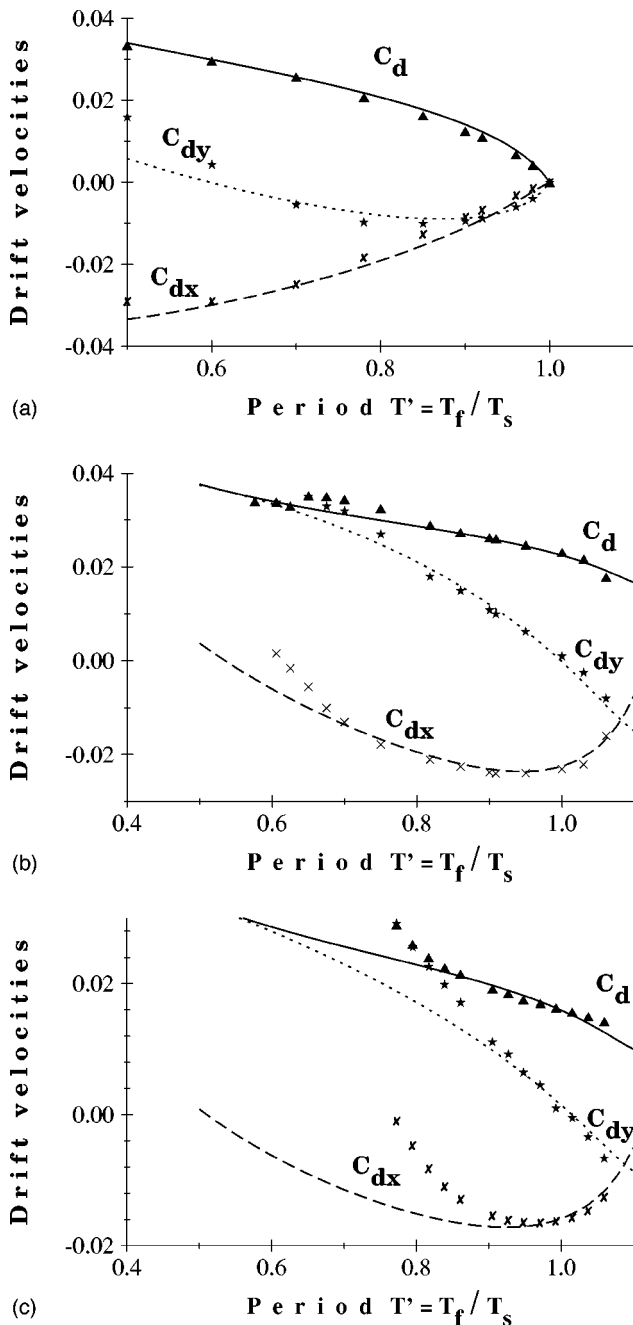


FIG. 6. Comparison of numerical results (points) and the phenomenological model (10) (lines). In (a)–(c) cases A–C from Fig. 1 are shown, respectively. Parameters for the phenomenological model are  $\lambda=0.0$  and  $\vartheta=40.0$  for case A,  $\lambda=7.4$  and  $\vartheta=83.0$  for case B, and  $\lambda=3.7$  and  $\vartheta=57.0$  for case C.

$$\begin{aligned}
 c_{dx} &= \frac{R(\cos(\omega\varphi) - \cos(\omega\vartheta)) + \lambda \sin(\omega\varphi)}{T_c^* - (\lambda/c_f)\cos(\omega\varphi)}, \\
 c_{dy} &= \frac{R(\sin(\omega\varphi) - \sin(\omega\vartheta)) - \lambda \cos(\omega\varphi)}{T_c^* - (\lambda/c_f)\cos(\omega\varphi)}.
 \end{aligned}
 \tag{10}$$

The extremely sparse limit (1) is obtained for  $\lambda = \vartheta = 0$ .

Figure 6 shows a comparison of the numerically obtained drift velocities and our formula (10). For large  $T'$  the phenomenological model fits the numerical data very well. As already mentioned in Sec. III, we observe for small  $T'$  a

different drift behavior due to the interaction of the stimulating wave fronts themselves. There we do not expect the model (10) to be valid. Moreover, from a clinical point of view the focus is on large  $T'$ .

In the remainder we motivate the reduction of the tip movement and the resulting formulas (9) and (10).

The reduced trajectory on the circle BC is motivated by the observation that during phase 3, as mentioned earlier, the tip moves with the velocity  $c_s$ . Therefore, the free parameter  $\theta$  allows us to map the real motion during phases 3 and 4 onto the circle. We denote the travel time of the spiral tip on this circle from B to C by  $T_c^*$ . As can be seen from Fig. 5(b),  $T_c^*$  is implicitly given by

$$c_f(T_c^* - T_f) = R \sin(\omega(T_c^* - \vartheta)) - R \sin(\omega\vartheta). \tag{11}$$

Note that the extremely sparse limit (2) is recovered for  $\vartheta = 0$  [see Eq. (1)].

The displacement of the circle, i.e., the motion along the straight line AB, is modeled by the second free parameter  $\lambda$ . The movement along the straight line AB corresponds to the noncurling phase 2. During this noncurling phase the tip velocity in the  $y$ -direction is  $c_f$ , as mentioned earlier. The displacement AB depends on the initial phase 1 and the noncurling phase 2. We will lump these phases together into a main drift. We assume that the movement of the tip after the collision will, as a lowest-order approximation, follow the initial line of the inhibitor since, as a general rule, a wave tip will move into a region where it can do so. We assume that the direction of the mean drift is given by the direction of the inhibitor at the time of collision. Considering moderately dense spirals, this direction is tangential to the core. From Fig. 5(a) it follows that the  $x$ -displacement during the mean drift is  $\lambda \sin(\omega\varphi)$  and the  $y$ -displacement is  $-\lambda \cos(\omega\varphi)$ .

### VI. DRIFT OF MEANDERING SPIRALS

Meandering naturally occurs if the density of a spiral wave is increased. The core then does not move along one circle with a well-defined radius, but instead moves along petals whose centers are lined up on a large circle with radius  $R_L$ . With the petals one can associate a smaller radius  $R_S$ , as shown in Fig. 7(a). When increasing the density, first inwards petals are observed and, with further increase of excitability, outward petals. The onset of meandering has been studied in Refs. 19 and 20.

Our main result is that a meandering spiral drifts like a nonmeandering spiral, when periodically stimulated. Numerical calculations demonstrated that meandering spirals are exposed to the same drift mechanisms as nonmeandering spirals. A meandering spiral, as shown in Fig. 7(a), drifts under influence of periodic stimulation rectilinearly [Fig. 7(b)]. Movement of a freely meandering spiral along a straight line is well known and has been observed. But there, the larger radius  $R_L$  is only infinite for one special value of the control parameter. In fact, this value of the control parameter separates the phases of inward and outward growing petals. The drift we observe here is different from this sce-

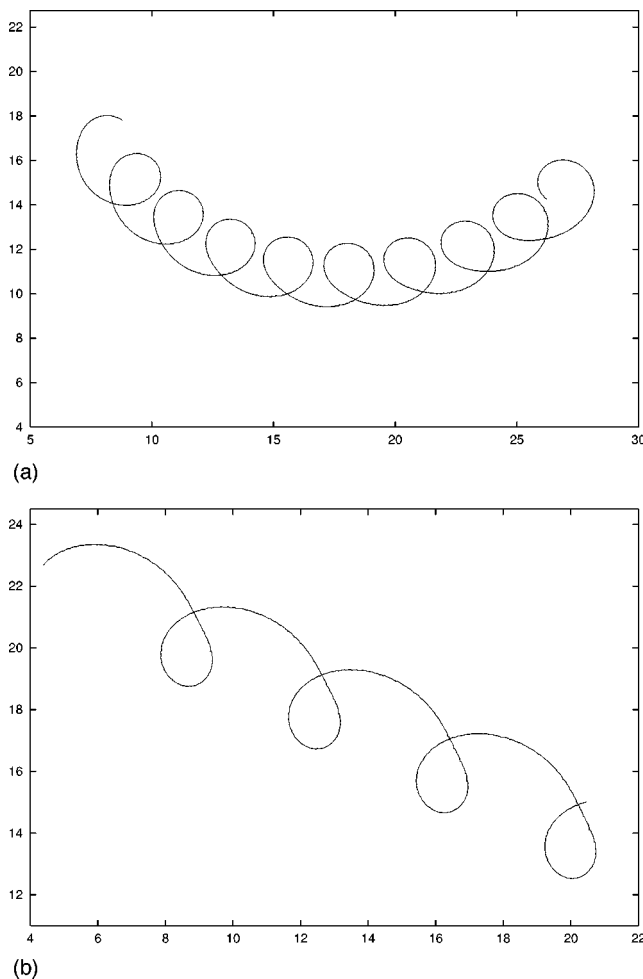


FIG. 7. Trajectories of the tip of a meandering spiral. (a) Freely meandering spiral with two clear defined radii. (b) Same under the influence of a stimulating periodic wave train coming from the lower boundary. Parameters are those of case C in Fig. 2.

nario and is robust in the sense that it does not depend on the particular values of the control parameters, but is instead a generic situation.

For meandering spirals, again we are faced with nonzero drift velocities for stimulation periods larger than  $T_s$  [see Figs. 2(a)–2(c), case C]. If  $T_s$  is taken to be the time between two consecutive points of equal phases of the freely meandering spiral, i.e.,  $T_s$  is associated with the smaller radius  $R_S$ , and  $R$  is taken to be the smaller of the two radii  $R = R_S$ , formulas (9) and (10) are in good agreement with the numerical simulation (Fig. 6).

Free meandering itself is a strongly nonstationary process where the spiral wave tip moves periodically into its own refractory tail. On the smaller circle the excitability is high and the spiral curls. It will meet its own refractory tail and moves into an area with low excitability where it continues to move on a large circle with  $R_L$  until an inhibitor-free hole opens and the wave tip can freely curl again with its growing velocity. Hence, meandering is basically due to the fact that the spiral wave periodically changes the excitability of the medium it moves through by its own inhibitor. Periodic stimulations such as the emission of wave trains drastically change the excitability of the active medium and dis-

turb this inherent periodicity of the spiral wave and impose their own periodicity. This suppresses and transforms the meandering and a steady drift will be established. Barkley<sup>20</sup> has identified the Euclidean symmetry group as being essential for the onset of meandering. The invariance under the action of the Euclidean group, rotation, reflection, and translation leads to a reduction of the original system to a set of five ordinary differential equations. In this system, the onset of meandering is described by a Hopf bifurcation. The periodic stimulation by wave trains does break the symmetry and destroys the meandering.

## VII. DISCUSSION

We have investigated drift of spiral waves induced by a periodic wave train which is launched close to the core. The surprising result of nonzero drift velocities for stimulating periods larger than the period of the freely rotating spiral has been observed. We note that for stimulations far from the core the spiral wave arms shield the core and will prevent a drift of the core, but once a drift has been induced by a stimulation close to the core, this drift will be stationary. This seems to contradict the conclusions of former work.<sup>4,5</sup> We found that a transitory phase caused by an interaction of the wave train with the refractory tail of the spiral wave is responsible for this new phenomenon. Essentially this transitory phase introduces a larger spiral wave period and hence allows for stimulating periods larger than the original spiral wave period  $T_s$ . A phenomenological model was established which quantitatively describes the drift velocities for moderately sparse spirals. Initially meandering spirals were also stimulated and we observed a steady drift along a straight line as in the nonmeandering cases. The stimulation by wave trains does dominate the inherent periodic nature of meandering spirals. We could again describe the drift with our phenomenological formula.

The new result of nonzero drift for stimulation periods larger than  $T_s$  was mainly due to two separate factors: (i), we leave the parameter region of extreme densities and (ii), we stimulate close to the core. In the remainder we comment on these two issues and put them into a perspective from a clinical point of view.

Considering stimulations close to the core is relevant from a cardiological point of view. Here typical wave velocities are of the order 10 cm/s and typical time scale is of the order of 0.2 s, which implies a typical wavelength of 2 cm, which is not too small if compared with the heart size. In this case obvious general collision arguments, as employed in the aforementioned classical theories, do not apply. Nevertheless, we saw that for the case of extremely sparse spirals there is no drift for  $T_f > T_s$  also in the case where the source of stimulation is close to the core [case A in Figs. 2(a)–2(c)]. After one initial collision and the resulting displacement of the core, the spiral wave arm develops and starts shielding the core. For moderately sparse spirals, though, we do observe nonzero steady drift velocities for  $T_f > T_s$ . This brings us to the problem of the density of spirals.

The density  $\delta$  of a spiral can be defined as the ratio of the width of the spiral wave arm and the wavelength of the

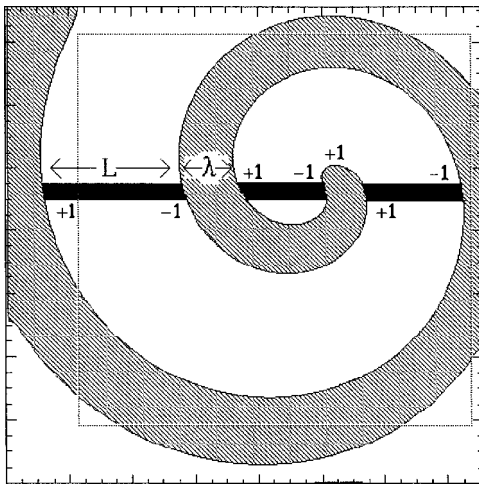


FIG. 8. Spiral wave and a stimulating front (black filled). The shaded area depicts the space occupied by the spiral and its refractory tail. At the intersection of the planar front and the spiral wave the topological charge of the resulting broken end is denoted. The dashed box shows a possible boundary of the medium.

spiral wave. In other words, the density is a measure of the ratio of the space already occupied by the spiral to the space that would still be available for excitations. The density is particularly important for defibrillation. It determines the excitable gap, i.e., the probability of intersections of the stimulating front with the spiral wave at the moment of stimulation. Hence it determines the number of newly created broken fronts which eventually may evolve into new spiral wave arms. As a consequence, the mechanism is one whereby spirals drift strongly depends on density. In fact, excitation by wave trains may worsen the situation by not annihilating the existing spiral (or moving its core into non-excitable tissue) but by creating even more spiral waves. In the Appendix we derive an expression for the success rate of defibrillation depending on the density.

#### APPENDIX: DENSITY DEPENDENCE OF SUCCESS RATE

In this appendix we employ an argument based on the conservation of the topological charge  $N$  to find an expression for the success rate  $P_s(\delta)$  of defibrillation induced by stimulating wave trains. As shown in Fig. 8, we assume stimulation with a planar front. The intersection of the boundary of the excitable medium with the stimulating front can lay either on fresh medium or on a spiral wave arm or its refractory zone. This determines the number of broken ends created by the stimulating front, and hence the overall topological charge. We define the topological charge  $N$  to be  $+1$  for counter-clockwise rotating spirals,  $-1$  for clockwise ro-

tating spirals, and  $0$  if no broken end at all is present. Topological charges add up, so two counter-rotating spirals with  $N=1$  and  $N=-1$ , respectively, result in  $N=0$ , which expresses the fact that they are very likely to annihilate each other (only for the case of equal rotation frequencies they may coexist). If only one spiral wave is present with an initial charge  $N=+1$  as depicted in Fig. 8, the sum of topological charges may be either  $0$ ,  $+1$ , or  $2$  depending on the four possibilities for the location of the boundaries. If  $N=0$ , complete annihilation is observed. If  $N=+1$ , we are able to induce spiral wave drift with stimulating wave trains as discussed in this article and force the spiral wave with  $N=+1$  out of the boundary. If  $N=+2$ , the stimulation has actually created an additional spiral wave with the same sense of rotation, so fibrillation is enhanced.

The probability  $P_r$  for one boundary being located on a spiral wave arm or its refractory zone is  $P_r = \lambda / (L + \lambda) = \delta$ .  $P_f = 1 - \delta$  is then the probability for an intersection of the boundary with fresh medium.

The success rate  $P_s$  is naturally defined as the sum of the probability for complete annihilation  $N=0$  and of the probability for possible induced drift  $N=+1$ . Simple counting of topological charges for all four possibilities for the location of the boundaries leads to

$$P_s = (1 - \delta)^2 + \delta. \quad (\text{A1})$$

In particular, this implies that  $P_s > 0.75$  for all  $\delta$  and that for spiral waves with  $\delta = 0.5$  the success rate is the worst.

<sup>1</sup>A. T. Winfree, *Science* **266**, 175 (1972).

<sup>2</sup>F. Siegert and C. Weijer, *Physica D* **49**, 224 (1991).

<sup>3</sup>J. M. Davidenko, A. M. Pertsov, R. Salomonsz, W. Baxter, and J. Jalife, *Nature (London)* **335**, 349 (1992).

<sup>4</sup>V. I. Krinsky and K. I. Agladze, *Physica D* **8**, 50 (1983).

<sup>5</sup>Ye. A. Yermakova, V. I. Krinsky, A. V. Panfilov, and A. M. Pertsov, *Biophysics (Engl. Transl.)* **31**, 348 (1986).

<sup>6</sup>M. Vinson, *Physica D* **116**, 313 (1998).

<sup>7</sup>M. Markus, Zs. Nagy-Ungvaray, and B. Hess, *Science* **257**, 225 (1992).

<sup>8</sup>M. Vinson and A. M. Pertsov, *Phys. Rev. E* **59**, 2764 (1999).

<sup>9</sup>K. I. Agladze, V. A. Davydov, and A. S. Mikhailov, *Pis'ma Zh. Eksp. Teor. Fiz.* **45**, 601 (1987).

<sup>10</sup>V. A. Davydov, V. S. Zykov, A. S. Mikhailov, and P. K. Brazhnik, *Izv. Vyssh. Uchebn. Zaved., Radiofiz.* **31**, 574 (1988).

<sup>11</sup>A. P. Muñuzuri, C. Innocenti, J.-M. Flesselles, J.-M. Gilli, K. I. Agladze, and V. I. Krinsky, *Phys. Rev. E* **50**, 667 (1994).

<sup>12</sup>D. Barkley, *Physica D* **49**, 61 (1991).

<sup>13</sup>A. M. Pertsov, E. A. Ermakova, A. V. Panfilov, *Physica D* **14**, 117 (1984).

<sup>14</sup>A. M. Pertsov, J. M. Davidenko, R. Salomonsz, W. Baxter, and J. Jalife, *Circ. Res.* **72**, 631 (1993).

<sup>15</sup>A. V. Panfilov and J. P. Keener, *J. Theor. Biol.* **163**, 439 (1993).

<sup>16</sup>G. Huyet, C. Dupont, T. Corriol, and V. Krinsky, *Int. J. Bifurcation Chaos Appl. Sci. Eng.* **8**, 1315 (1998).

<sup>17</sup>A. Pumir and V. Krinsky, *J. Theor. Biol.* **199**, 311 (1999).

<sup>18</sup>V. N. Biktashev and A. V. Holden, *Phys. Lett. A* **181**, 216 (1993).

<sup>19</sup>V. Hakim and A. Karma, *Phys. Rev. E* **60**, 5073 (1999).

<sup>20</sup>D. Barkley, *Phys. Rev. Lett.* **72**, 164 (1994).